Investigating the Effect of the Deep Cryogenic Heat Treatment on the Mechanical Properties and Corrosion Behavior of 1.2080 Tool Steel

K. Amini [1*] , A. Akhbarizadeh [2], S. Javadpour [3]

[1] *Department of Mechanical Engineering, Tiran Branch, Islamic Azad University, Isfahan, Iran.*
[2] *Department of Materials Science and Engineering, Shiraz Branch, Islamic Azad University, Shiraz, Iran.*
[3] *Department of Materials Science and Engineering, Shiraz University, Shiraz, Iran.*

Abstract

Deep cryogenic heat treatment is assumed as a supplementary heat treatment performed on steels before the final tempering treatment to enhance the wear resistance and hardness of the steels. In this study, the effects of the deep cryogenic heat treatment on the wear behavior and corrosion resistance of the 1.2080 tool steel were studied using the wear testing machine and polarization and impedance spectroscopy tests. Moreover, the microstructural changes of the deep cryogenically treated samples were clarified via the scanning electron microscope (SEM) and X-ray diffraction testing machine. The results showed that the deep cryogenic heat treatment eliminated the retained austenite and made a more uniform carbide distribution with higher percentages. Beyond this, it was clarified that the deep cryogenic heat treatment increased the hardness and improved the wear behavior of the 1.2080 tool steel, as well as decreasing the corrosion resistance, due to the higher chromium carbides produced during the deep cryogenic heat treatment.

Keywords: Deep cryogenic heat treatment; Wear behavior; Corrosion resistance; Microstructural changes.

Introduction

Cryogenic heat treatment was introduced to the industries in the second decade of 20th century. This special kind of the supplementary heat treatment plays an important role in selecting the finishing production procedure of parts with the lowest wear rate, lowest austenite percentage, and the most economic costs [1, 2]. This specific heat treatment is divided into two different groups: (i) Shallow cryogenic heat treatment performed at temperatures higher than 125 K, and (ii) deep cryogenic heat treatment in which samples are cooled to the lower temperatures (125–77 K) [3]. The main effect of the cryogenic heat treatment is the elimination of the retain austenite due to decreasing the sample temperature below the martensite finish (Mf) one. Beyond this, the deep cryogenic treatment reduces the chromium carbides size, increases its percentage, and makes a more homogenized carbide distribution [4, 5]. These microstructural changes are a consequence of carbon atoms jumping at the lower temperatures, because of the high degree of contraction in the martensite structure at those temperatures. These carbon atoms jump to the neighboring sites, acting as an appropriate place for the eta chromium carbide nucleation in the prior tempering [6]. These new carbides increase the carbides percentage and make a better carbide distribution in the material after the deep cryogenic treatment [7]. The deep cryogenic heat treatment is performed on a wide variety of materials, including carburized steels, high speed steels, composites and polymers and the tool steels, which are the most interesting area of research [4, 5]. A lot of studies have been conducted on tool steels including M, O, T and D series. One of the most attractive research areas in tool steels is D series due to their role and popularity in die-making [8]. Investigations have shown that the deep cryogenic heat treatment improves the hardness and the wear behavior of the tool steels [9- 12]. Despite these studies, there is lack of investigations addressing the effect of the deep cryogenic heat treatment on the corrosion behavior of the tool steels. For this purpose, this study focused on the wear behavior and corrosion resistance of the deep cryogenically treated 1.2080 (D3) tool steels via the in on disk testing machine, polarization tests and the electrochemical impedance spectroscopy.

** Corresponding author:*
Tel: +98 913 165 1659, Fax: +98 42 22 9150
Email: Kamran_amini1978@hotmail.com
Address: Department of Mechanical Engineering, Tiran Branch, Islamic Azad University, Isfahan, Iran.
1. Associate Professor
2. Associate Professor
3. Professor

2. Materials and Methods

A commercial 1.2080 (D3) tool steel bar with the diameter of 20 mm was cut into disks with the height of 5 mm. The composition of the bar was analyzed via ARL 3460 Computerized Optical Emission Quantometer System (OES) (Table 1).

Table 1 .1.2080 tool steel nominal composition.

Elements	wt.%
C	2.2
Si	0.6
Mn	0.6
V	0.5
Cr	12
W	0.4
Fe	Remaining

For conventional heat treatment, the samples were austenitized in an Exiton electrical furnace at 950 ºC for 15 min and then quenched in oil. The conventionally treated samples were named CHT ones. For cryogenic heat treatment, the samples were cooled down to -195 ºC, held at that temperature for 24 hours and then warmed up to room temperature with the cooling and heating rate of 5 ºC/min. These samples were named deep cryogenically treated samples, DCT ones. After that, all samples were tempered at 180 ºC for 3 h in an electric oven.

After heat treatment and tempering, all samples were grounded up to the number 1000 grinding paper and this was followed by polishing via alumina (0.5 µm) to reach a smooth and uniform surface. One sample in each group was selected randomly and analyzed via XRD.

X-ray diffraction (XRD) with cu Kα radiation was used to clarify the phases and the retained austenite percentage. The XRD analysis of the samples showed that in addition to the austenite and martensite, chromium carbide existed in the structure. The retained austenite percentage was calculated with respect to ASTM E975-13 standard [13]. The combination of the phase's percentage should be equal to 100%. The carbide percentage was evaluated via the SEM micrographs and the austenite percentage was calculated according to Eq. 1:

$$V_\gamma = \left[\frac{(1-V_C)(I_\gamma / R_\gamma)}{(I_\alpha / R_\alpha)} + (I_\gamma / R_\gamma) \right] \quad \text{Eq. (1)}$$

, where and are the retained austenite and carbide percentage, respectively; and are the integrated intensity per angular diffraction peak (hkl) in the austenite and martensite phases, respectively. Also, and are the austenite and martensite constants, respectively. The value of R can be calculated with respect to the (hkl) plane in combination with the polarization, multiplicity and structure factor of the phases according to the ASTM E975-13 standard.

For microstructural analysis, the samples surface was analyzed via the scanning electron microscope (SEM, Oxford Instrument Stereoscan 120 and SEM VEGA\ TESCAN) to clarify the carbides in the structure. These micrographs could be used to evaluate the carbides percentage and determine their distribution. To study the microstructural changes of the samples, the samples surface was etched in (a) 100 ml H_2O, 10 g $K_3Fe(CN)_6$ and 10 g NaOH, (b) Mixed acid (3 ml HF, 53 ml H_2NO_3, 2 ml CH_3COOH and 42 ml H_20), and (c) Nital 4% (96 ml ethanol and 4 ml HNO_3). The samples were etched in each of these etchants for 2 s 3–4 times. This combination only clarified the carbides and did not affect other phases. The carbide content was calculated from optical microscopy micrographs using some image analyzing software (Clemex Vision, version 3.5.025).

Microhardness testing was carried out using a COOPA MH1 microhardness tester equipped with a Vickers indenter under a load of 500 gf and a load exertion time (dwell time) of 15s to calculate the hardness variation of the samples. The wear tests were carried out with a pin-on-disk wear tester equipped with steel pins with the hardness of 68 HRC, according to the ASTM G99-05(2010) standard. The wear tests were carried out at 25±5 ºC with 30±10% humidity and the applied loads of 110 and 160N in three sliding velocities of 0.05, 0.1 and 0.15 m/s. The sliding distance was 1000 m and the samples weight loss was calculated via an electronic balance with an accuracy of 0.0001 gr. The wear rate was calculated by Eq. 2:

$$Wr = \Delta m/(\rho LFN) \times 10^3 \quad \text{Eq. (2)}$$

, where Wr is the wear rate in mm^3/Nm, Δm is the weight loss in gr, ρ is the steel density in gr/cm^3, L is the wear distance in meter, and F_N is the load in Newton.

The corrosion resistance of the samples was determined using linear sweep voltammetry experiments. The polarization measurements were carried out with a scan rate of 1 mVs^{-1} using an Autolab potentiostat model type 3, EcoChemie BV, and some General Purpose electrochemical System 4.9 software. It was conducted in a 3.5 %wt. NaCl aqueous solution using a classic three-electrode cell with a platinum plate as the counter electrode and an Ag/AgCl electrode as the reference electrode. The

samples were cleaned in acetone and then drawn in deionized water before the electrochemical test. The samples were covered with lacquer so that only 1 cm^2 area was exposed to the electrolyte. The specimens were immersed in the mentioned solution for 120 min at room temperature to reach a steady state. After that, the samples were transferred into the test holder and then were allowed to remain there for 1500 seconds to calculate the OCP (Open Circuit Potential). The samples were then analyzed in the range of -250 mv to +250 mv with respect to the OCP [14, 15]. Icorr was then calculated with respect to anodic and cathodic branch of the Tafel test and via the extrapolating method [14,15]. Each test was carried out two to three times to reach a reliable average. The corrosion rate of the samples was analyzed according to Eq. 3:

$$MPY = i_{corr}(\Delta)(2/\rho)(\varepsilon) \quad \text{Eq. (3)}$$

, where Δ is a combination of several conversion terms and is 1.2866×10^5[euvalents.sec.mils]/[Colombs. cm.years]

ι_{corr} is the corrosion electric current in Amps/cm^2

ρ is denity in grams/cm^3

ε is equivalent weight in grams/equivalents [14].

For Cyclic analysis, the samples were examined in the range of -250 mv to +2 V with respect to the OCP.

For more accuracy, the electrochemical impedance spectroscopy (EIS) test was also performed in the frequency range of 0.001 to 100000 Hz and the voltage amplitude of 10 mV. The samples were analyzed via Autolab potentiostat model type 3, EcoChemie BV, and Fra software. After data fitting, the simulated circuit was evaluated via the experimental observations.

3. Results and Discussion

3.1. Microstructural analysis

The XRD analysis of the samples showed that the retained austenite was completely eliminated after the deep cryogenic heat treatment (Fig. 1). The retained austenite was reduced from 13 wt. % to below the detection limit of the XRD method (<1 wt. %). The eliminated retained austenite is highlighted in Fig. 1. The results also showed that in addition to austenite and martensite, chromium carbide also existed in the samples (Fig. 1). The SEM micrographs clearly showed that the carbide percentage was increased during the deep cryogenic heat treatment by 5%, from the 18 vol.% in the CHT sample to 23 vol.% in the DCT one (Fig. 2).

The SEM micrographs also clarified some newly formed carbides produced during the deep cryogenic heat treatment. Briefly, the deep cryogenic heat treatment increased the carbide percentage and made a more homogenous carbide distribution in the structure. It was also shown that the deep cryogenic heat treatment increased the number of carbide particles and decreased the carbides size, making a more homogenous carbide distribution due to the deep cryogenic heat treatment.

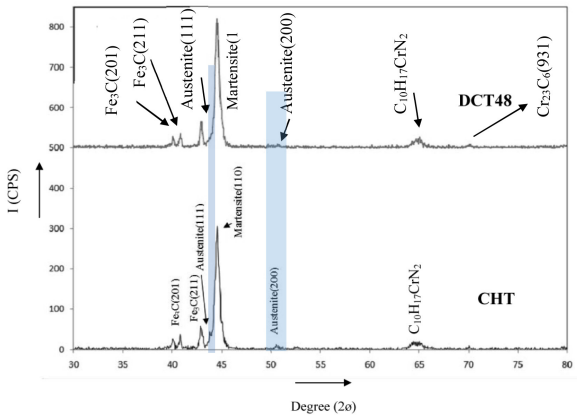

Fig.1. XRD pattern of the 1.2080 tool steel.

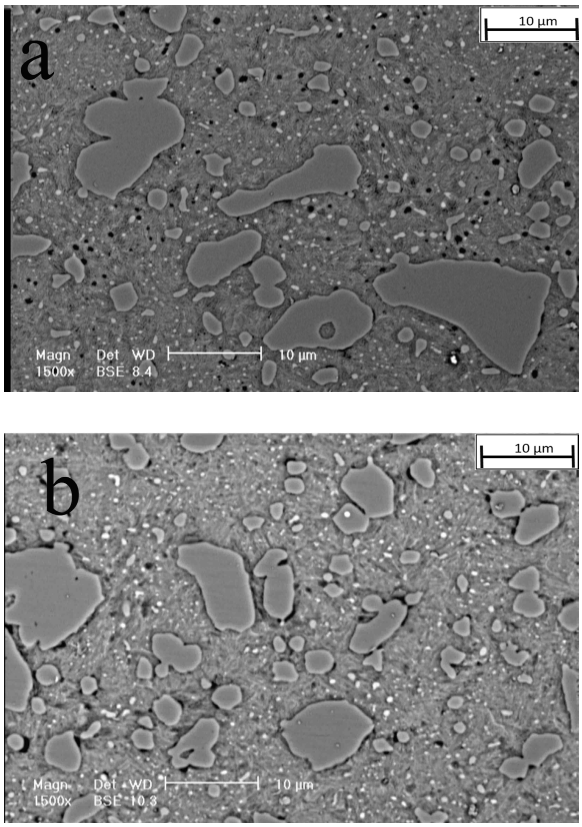

Fig. 2. SEM micrograph of the carbides in the (a) CHT and (b) DCT samples at 1500X.

During the deep cryogenic heat treatment, the structure endured a high degree of stresses due to the structure contraction at low temperatures and the different expansion coefficient of austenite and martensite. These high degrees of stresses forced carbon atoms to jump to the nearby defects. New defects were also produced due to the contraction and the different expansion coefficient of austenite

and martensite in the phase boundaries. These newly jumped carbon atoms acted as preferential new sites for the carbide nucleation in tempering [1,5,8]. In other words, martensite was decomposed and new carbides were produced.

Microhardness results showed that the deep cryogenic heat treatment considerably increased the microhardness from 920 MPa to 980 MPa in DCT sample. These results were in a good agreement with the microstructural observations, clarifying that the retained austenite as a soft phase was eliminated in the DCT samples. Moreover, the carbide percentage was increased and hence, the hardness was improved.

Pin- on- disk wear testing results also showed that the deep cryogenic heat treatment increased the wear resistance of samples in all sliding velocities and loads for 50-85% (Fig. 3). It was shown that the wear rate was decreased with increasing the sliding speed (3b). This increase in the wear rate was a consequence of severe surface contact between pin and disk, higher localized surface temperature, and the more powerful impact of pin junctions to the disk junctions at higher sliding velocities. Moreover, with increasing the applied load from 110 to 160 N, the wear resistance was not changed drastically; this was because in Eq. 2, the normal force at the denominator of the equation neutered the weight loss in the numerator (Fig. 3).

Potentiodynamic polarization curves of the conventionally and deep cryogenically treated samples in the 3.5 wt. % NaCl solution are shown in Fig. 4. It can be observed that deep cryogenic heat treatment declined the corrosion resistance of the 1.2080 tool steel for 54%. Table 2 shows that the deep cryogenic heat treatment changed the current densities to more positive values and also decreased the potentials to the lower values; hence, the corrosion rate of the DCT samples was increased, as compared with the CHT ones.

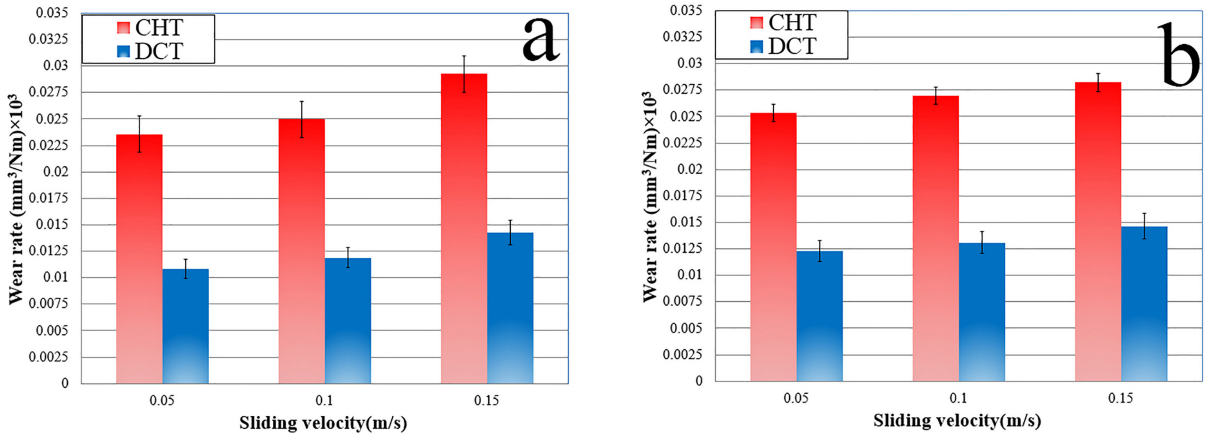

Fig. 3. Wear rate of samples at different sliding speeds of 0.05, 0.1 and 0.15 m/s under (a) 110 and (b) 160 N normal load after the sliding distance of 1000m.

Table 2. Calculated parameters for polarization diagram from different samples in 3.5 wt. % NaCl solution

Samples nomination	OCP (v)	i_{corr} (amp/cm^2)	β_c (V/ dec)	β_α (V/ dec)	E corr (v)	Corrosion rate (mm/year)
CHT	-0.467	0.000001323	0.112	0.067	-0.501	-0.592
DCT24	-0.592	0.000006	0.077	0.115	-0.592	0.0694

The Impedance spectroscopy of the CHT and DCT samples is shown in Fig. 5. The equivalent electrical circuit of the samples was drawn; it was clarified that all samples showed a one capacitive loop (Fig. 5d). In this diagram, the Rs is the solution resistance between the sample and the reference electrode, R_1 is the charge transfer resistance, C is the double layer capacitance, and n shows the deviation from ideal capacitance (n=1). The size of the loop is a function of the corrosion resistance of the samples. In other words, increasing the loop diameter led to a decrease in the corrosion rate [16]. Similarly, the diameter of the loop showed the charge transfer resistance. The loop of the DCT samples was smaller than that of the CHT ones and hence, the corrosion rate was increased due to the deep cryogenic heat treatment (Fig. 5). The calculated parameters of impedance diagram are shown in Table 2. This behavior was a consequence of

carbide precipitation during the deep cryogenic heat treatment. During the deep cryogenic heat treatment, the structure endured a high degree of stresses due to the structure contraction at low temperatures and a different expansion coefficient of austenite and martensite.

This phenomenon forced carbon atoms to jump to the nearby defects. During the deep cryogenic treatment, the structure was contracted and some new defects including dislocations, twins, etc. were created. These defects, in cooperation with the old defects, attracted carbon atoms from the saturated and contracted martensite structure. These atoms would act as the preferential sites for carbide nucleation during the former tempering. These newly formed carbides could increase the carbide percentage and make a more homogenous distribution [1, 4, 8].

Increasing the carbide percentage would lead to a decrease in the solutionized chromium atoms in the structure. The chromium atoms are the major elements in increasing the corrosion resistance of the steels. The chromium atoms can considerably improve the corrosion resistance when they exist in the structure as the free atoms to produce the protective oxide film [17, 18]. Deep cryogenic heat treatment decreased the free chromium atoms and subsequently, declined the corrosion resistance noticeably (Tables 2 and 3). Beyond this, increasing the carbides percentage could lead to an increase in chromium carbide grain boundaries which would act as the galvanic cell during the corrosion. The grain boundaries were the high energy areas and hence, increasing the grain boundaries would to an increase in the corrosion rate of the deep cryogenically treated samples.

Hence, the corrosion rate of the samples with fine carbides was increased due to the more grain boundaries as potential sites for increasing the corrosion rate. These two phenomena increased the corrosion rate of the DCT samples, as compared with CHT ones.

For more studies, the cyclic test was also performed on the samples to show the corrosion behavior more accurately (Fig. 6). It was clarified that the pitting was the predominant corrosion mechanism in 3.5 wt. % NaCl solution. Beyond this, the passivation was not observed in the samples due to the low dissolved content of chromium as well as the low corrosivity of the test environment.

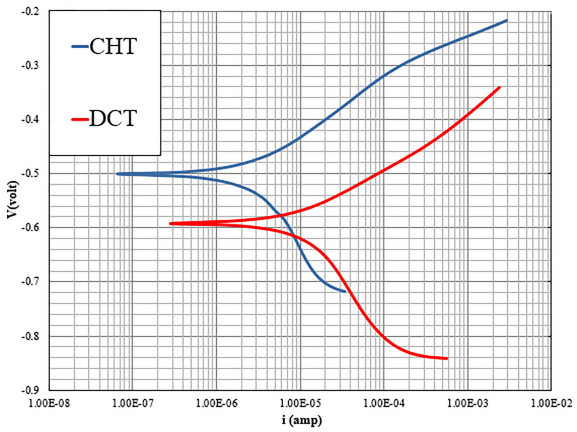

Fig. 4. Polarization curve of samples at different holding durations in 3.5 wt. % NaCl solution.

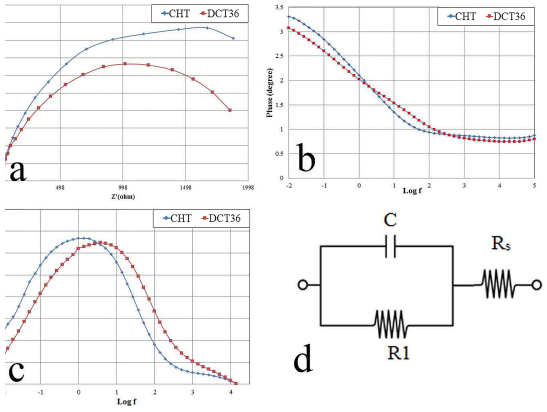

Fig. 5. Electrochemical spectroscopy diagram of CHT and DCT samples: (a) Nyquist plots, (b) bode phase angle, (c) bode impedance, and (d) equivalent circuit.

Table 3. Calculated parameters from impedance spectroscopy in 3.5 wt. % NaCl solution.

Samples nomination	**R_1(ohm)**	**Q(F)**	**R_s(ohm)**	**n**	**R_1+Rs(ohm)**
CHT	2397	0.001816	7	0.8049	2404
DCT24	2150	0.001987	7.11	0.8374	2157.11

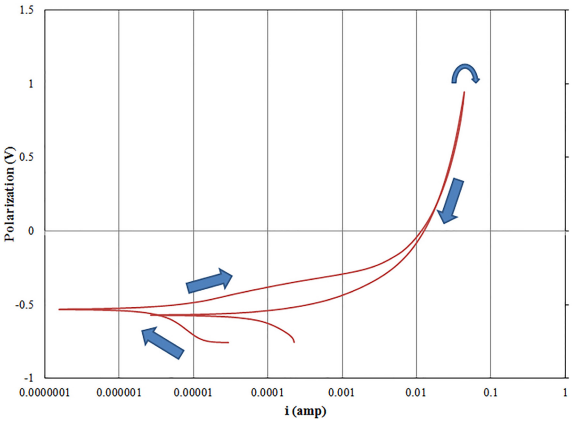

Fig. 6. Cyclic polarization curve of DCT sample.

4. Conclusion

This study was carried out to investigate the effect of the deep cryogenic heat treatment on the microstructure, hardness, wear behavior and corrosion resistance of the DIN 1.2080 tool steel. The following conclusions could be drawn from this study:

- The deep cryogenic heat treatment eliminated the retained austenite from 8% in the CHT sample to less than the detection limit of XRD. Furthermore, the carbide percentage was increased by 5%. Moreover, the deep cryogenic heat treatment made a more homogeneous carbide distribution. These improvements increased the microhardness for 12% in the deep cryogenically treated samples.
- Deep cryogenic treatment formed new fine carbides that had different sizes varying from micron to nano-sized dimensions. These newly formed fine carbides increased the hardness of the samples and improved the wear behavior of the 1.2080 tool steel.
- The wear behavior was improved during the deep cryogenic heat treatment for 50-85%. This improvement was a result of a more uniform carbide distribution, the retained austenite elimination, and an increase in the carbide percentage.
- It could be observed that deep cryogenic heat treatment declined the corrosion resistance of the 1.2080 tool steel for 54%. This behavior was a consequence of decreasing the dissolved chromium atoms in the structure of the DCT samples and increasing the martensite/chromium carbide grain boundaries as the potential sites for increasing the corrosion rate.

References

[1] N. S. Kalsi, R. Sehgal, V. S. Sharma: Mater. Manuf. Process., 25(2010), 1077.
[2] S. Kalia: J. Low Temp. Phys., 158(2010), 934.
[3] A. Akhbarizadeh, A. Shafyei, M. Golozar: Mater. Design., 30(2009), 3259.
[4] K. Amini, A. araghi, A. Akhbarizadeh: Acta Metall. Sin. (English Letters), 28 (2015), 348.
[5] W. Reitz, J. Pendray: Mater. Manuf. Process., 16(2001), 829.
[6] K.Amini, S. Nategh, A. Shafyei, A. Rezaeian: Int. J. Min. Met. Mater., 19(2012), 30.
[7] A. Akhbarizadeh, K. Amini, S. Javadpour: Mater. Design.,35 (2012), 484.
[8] H. Paydar, K. Amini, A. Akhbarizadeh: Kovove Mater., 52(2014), 163.
[9] K. Amini, A. Akhbarizadeh, S. Javadpour: I Int. J. Min. Met. Mater, 19(2012), 795.
[10] K. Amini, S. Nategh, A. Shafiey, M.A. Soltany : Proceedings of the 17Th International Metallurgical and Materials Conference, Czech Republic, 13-15 May 2008, 1.
[11] A. Akhbarizadeh, K. Amini, S. Javadpour: Mater. Design.,45(2013),103.
[12] C. H. Surberg, P. Stratton, K. Lingenhöle: 48(2008), 42.
[13] ASTM. Standard Practice for X-Ray Determination of Retained Austenite in Steel with Near Random Crystallographic Orientation. West Conshohocken, PA: ASTM International; 2013.
[14] W. S. Tait. An Introduction to Electrochemical Corrosion Testing for Practical Engineers and Science. Madison, Wis, USA: Pair O Docs Professionals; 1994.
[15] M. E. Orazem, B. Tribollet. Electrochemical Impedance Spectroscopy. Hoboken, New Jersey, USA: A John Wiley & Sons Inc; 2008.
[16] D. Song, A. B. Ma, J. H. Jiang, P. H. Lin, D. H. Yang: Trans. Nonferrous Met. Soc. China, 19(5) 2009, 1065.
[17] J. R. Davis. Stainless Steels. Materilas park, OH. USA: ASM International; 1994.
[18] R. A. Lula, J. G. Parr. Stainless steel. revised, illustrated ed. Michigan, USA: American Society for Metals; 2007.